

Structure of the Amino-Terminal Protein Interaction Domain of STAT-4

Uwe Vinkemeier, Ismail Moarefi,* James E. Darnell Jr., John Kuriyan†

STATs (signal transducers and activators of transcription) are a family of transcription factors that are specifically activated to regulate gene transcription when cells encounter cytokines and growth factors. The crystal structure of an NH₂-terminal conserved domain (N-domain) comprising the first 123 residues of STAT-4 was determined at 1.45 angstroms. The domain consists of eight helices that are assembled into a hook-like structure. The N-domain has been implicated in several protein-protein interactions affecting transcription, and it enables dimerized STAT molecules to polymerize and to bind DNA cooperatively. The structure shows that N-domains can interact through an extensive interface formed by polar interactions across one face of the hook. Mutagenesis of an invariant tryptophan residue at the heart of this interface abolished cooperative DNA binding by the full-length protein *in vitro* and reduced the transcriptional response after cytokine stimulation *in vivo*.

The STATs constitute a family of transcription factors that are necessary for the activation of distinct sets of target genes in response to cytokines and growth factors (1). The STAT proteins are activated in the cytoplasm by phosphorylation on a single tyrosine residue (2). Each STAT molecule contains an SH2 domain, and reciprocal SH2-phosphotyrosine interactions between two STAT molecules result in the formation of active dimers that translocate to the nucleus and activate gene expression (Fig. 1A) (2). The canonical recognition site for a STAT dimer encompasses 9 to 10 base pairs (TTCN₃₋₄GAA) of DNA (3). However, analysis of the binding of activated STATs to DNA targets revealed that the STAT binding sites can extend over two or more adjacent canonical sites (4, 5).

Mammalian transcription factors activate transcription and achieve biological specificity through interactions with other transcription factors, trans-activators, or the general transcription machinery (6). Although the molecular basis for these phenomena is poorly understood, direct protein-protein interactions among multiple promoter-bound proteins appear to mediate this synergistic activation (7). In the case of the STATs, a small NH₂-terminal domain mediates a number of

important protein-protein interactions that influence STAT function (8). This domain allows cooperative interactions between STAT dimers bound to adjacent target sites on DNA, leading to a prolonged half-life of the protein-DNA complex (9). Functional assays exploring transcriptional regulation of the hepatic Spi

2.1 gene revealed the necessity for cooperative STAT binding to two adjacent recognition sites for a full growth hormone response (10). These cooperative contacts also affect the binding site selection of different STATs on a natural promoter that contains multiple potential STAT recognition sites (4). Deletion of the NH₂-terminal ~100 residues of STAT-1 or STAT-4 abolishes cooperative binding to DNA (4, 9). The truncated protein fully retains binding to a single target site as a dimer, suggesting that the N-domain is dispensable for dimer formation and DNA binding (9), but is necessary for interaction between STAT dimers and binding site discrimination (4). The N-domain of STAT-1 is also required for interaction between STAT-1 and the transcriptional coactivator protein CBP, a large (~2500 amino acids) polypeptide with transacetylase activity (11). Additionally, the amino-terminal region of STAT-2 is involved in binding to the intracellular region of the interferon- α receptor (12).

The NH₂-terminal 131 residues of STAT-1 form a stable domain that is readily cleaved off the intact molecule, indicating that it is an independently folded mod-

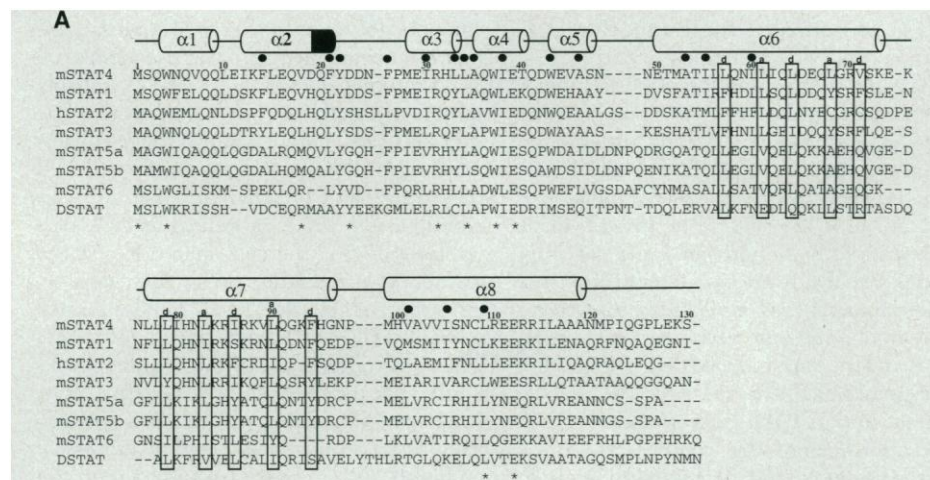
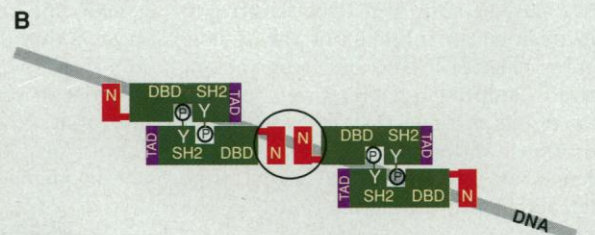


Fig. 1. (A) Sequence alignment of the conserved N-domain of the STAT family and secondary structure of STAT-4 (27). Human (hSTAT), murine (mSTAT), and *Drosophila* (DSTAT) proteins are included. The numbering is according to STAT-4. α -Helices α 1 to α 8 are drawn as cylinders. The blackened part of helix α 2 indicates a 3₁₀ helix. Invariant residues are highlighted with an asterisk below the alignment. Conserved residues in the hydrophobic core are marked with filled circles above the STAT-4 sequence. Residues in helices α 6 and α 7 that contribute to the packing of the coiled-coil are boxed, and their position in the helical repeats is indicated (a or d). **(B)** Schematic representation of two STAT dimers bound to adjacent target sites. Interactions between N-domains (N, circled) allow the dimers to bind to each other. Phosphotyrosines are indicated by Y attached to encircled P symbols. DBD, DNA binding domain; SH2, SH2 domain; TAD, transactivation domain.



U. Vinkemeier, Laboratory of Molecular Cell Biology and Laboratories of Molecular Biophysics, The Rockefeller University, New York, NY 10021, USA.

I. Moarefi and J. Kuriyan, Howard Hughes Medical Institute and Laboratories of Molecular Biophysics, The Rockefeller University, New York, NY 10021, USA.

J. E. Darnell Jr., Laboratory of Molecular Cell Biology, The Rockefeller University, New York, NY 10021, USA.

*Present address: Max-Planck-Institut für Biochemie, Abteilung für Zelluläre Biochemie, Am Klopferspitz 18, 82152 Martinsried, Germany.

†To whom correspondence should be addressed. E-mail: kuriyan@rockvax.rockefeller.edu

ule (9). Sequence alignments show that the N-domain is highly conserved (Fig. 1B). The average sequence identity for this region between mammalian STAT proteins is 40%, and ranges from 51% between STAT-1 and STAT-4 to 20% between STAT-5 and STAT-6. Over the ~750 amino acids that span the length of the common core of the STATs, only the SH2 domain is more highly conserved (13). The N-domain is also found in the *Drosophila* STAT (dStat92E) (Fig. 1B) (14) and in a recently discovered STAT in *Dictyostelium discoideum* (15). The first gene defect established in the DStat92E gene is a misspliced variant that produces both normal mRNA and an mRNA encoding only the NH₂-terminal 41 residues. Expression of this fragment has a partial dominant negative effect on transcriptional activation by the wild-type protein in cell culture and in the fly is associated with a weak abnormal phenotype (16).

We solved the crystal structure of the N-domain of STAT-4 (17) by multiwavelength anomalous diffraction and have refined an atomic model to a resolution of 1.45 Å ($R = 19.4\%$, $R_{\text{free}} = 22.3\%$) (Table 1). The STAT-4 N-domain is all helical, with an unusual architecture. Instead of the up-down connectivity of helix bundles or the box-like helical packing of the globin fold, the N-domain is constructed from three distinct structural elements that pack together. The NH₂-terminal 40 residues encompass the first four helices ($\alpha 1$ to $\alpha 4$), which form a ring-shaped element (colored red in Fig. 2 and Fig. 3B). A small helix ($\alpha 5$) connects this ring to the next structural element, an antiparallel coiled-coil formed by helices $\alpha 6$ and $\alpha 7$. The heptad repeat of hydrophobic amino acids, characteristic of coiled-coils,

is conserved across the STATs (Fig. 1B). Finally, the distal surface of the ring-shaped element forms a docking site for the last helix in the structure ($\alpha 8$). The overall appearance of the structure is that of a hook, with the inner surface of the hook being formed by the intersection of the proximal surfaces of the ring-shaped element and the coiled-coil. The N-domain of STAT-4 is dimeric in solution (18), and a twofold symmetry axis in the crystal generates a dimer with an extensive polar interface that involves one face of the hook.

The N-domain has a well-defined hydrophobic core that is conserved across the STATs, consistent with a stable and defined fold (Fig. 1B and Fig. 2). However, the NH₂-terminal ring-shaped element is stabilized by polar interactions involving buried charges. The ring is closed off by α helix-dipole interaction between the NH₂-terminal region of helix $\alpha 1$ and the carboxylate group of Glu³⁹, presented by the COOH-terminal region of helix $\alpha 4$ (Fig. 2B). Glu³⁹ forms a hydrogen bond with the amide nitrogen of residue Gln³ and is oriented correctly for this charge dipole interaction by the side chain of Arg³¹, which in turn forms a buried ion pair with Glu¹¹². Glu¹¹² is positioned by interactions with Tyr²² and a buried water molecule. Each of the side chains involved is invariant in all STATs (Fig. 1B), indicating that the ring-shaped element is conserved in architecture.

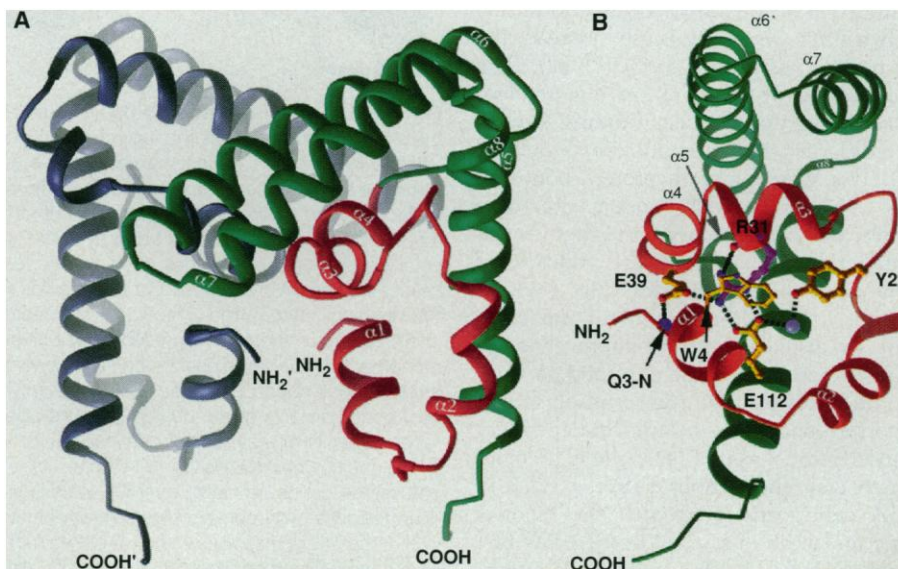
A consequence of the use of these polar groups in the ring-shaped element is the formation of a compact and potentially specific interaction surface. This structural element forms a relatively flat molecular surface that packs at an angle against another surface presented by the coiled-coil formed by helices $\alpha 6$ and $\alpha 7$. The juxta-

posing of the surface of the ring-shaped element with that of the coiled-coil results in a wedge-shaped groove. This groove is lined with hydrophobic residues, with polar residues at the center, and appears as though it could be a site of interaction with other proteins. A possible function for this groove is suggested by the fact that replacement of Arg³¹ or Glu³⁹ in STAT-1 by Ala results in a molecule that is more slowly dephosphorylated after interferon- γ induction than the wild-type protein (19). Thus, a phosphatase that controls STAT dephosphorylation might bind to the groove in the N-domain.

There is one molecule in the asymmetric unit of the STAT-4 crystal, and it is related to another by a twofold symmetry axis (Fig. 2A and Fig. 3A). There is an extensive interface between the two monomers of the dimer that buries 1714 Å² of surface area (Fig. 3A). An extended intermolecular hydrogen bonding network is formed at the interface that includes 15 amino-acid side chains and 12 water molecules per monomer (Fig. 3B). In addition, five backbone contacts are also observed in each monomer. Eleven of the 15 residues at the interface make direct hydrogen-bonding contacts to the other monomer. The water molecules at the interface are very well defined in the electron density map, and many of them have low temperature factors (<10 Å²) (Fig. 3C).

The interface between N-domain monomers is almost entirely polar. In contrast to the leucine zipper, wherein hydrophobic residues are used to generate the intermolecular interface by the formation of a coiled-coil across the dimer interface (20), the coiled-coil in the N-domain is firmly anchored within the domain and its role is to serve as an architectural support

Fig. 2. Tertiary structure of the N-domain of STAT-4. (A) Overall representation of two monomers (green and gray) in the crystallographic dimer, viewed approximately orthogonal to the molecular twofold axis, which is vertical. The ring-shaped NH₂-terminal element is colored red in one monomer. (B) Orthogonal view of one of the N-domains shown in (A), depicting details of the architecture of the ring-shaped element. Side chains that participate in a charge-stabilized hydrogen-bond network are shown in a ball-and-stick representation. The side chain and backbone carbonyl of buried R31 are shown in magenta. For clarity, the indole ring of the invariant residue W4 that seals off this arrangement on the proximal side is drawn with thinner bonds. The blue sphere denotes a buried water molecule. Hydrogen bonds are indicated by dotted lines. Oxygen, nitrogen, and carbon atoms are red, blue, and yellow, respectively. Q3-N marks the position of the backbone amide group of residue Q3. The light-red segment of helix $\alpha 2$ highlights its 3₁₀ helical conformation. Fig. 2 and Fig. 3, B and C were created with the program RIBBONS, version 2.0 (28).



for the presentation of a number of interacting side chains at the interface between N-domains and at the potential interaction groove. Whereas hydrophobic interactions are associated with stabilization of folded protein structures and are often found at the core of tight interfaces, polar interactions can provide both stability and specificity in protein-protein interactions (21). In contrast to the residues that constitute the buried core of the N-domain, which are conserved across STATs, the majority of the residues at the dimer interface are not conserved (Fig. 1B and Fig. 3B). This variation may provide specificity in STAT dimer-dimer interactions on DNA. Only two of the residues at the interface are invariant in all STATs: Trp³⁷, a central anchor residue at the interface, and Glu³⁹, which also participates in the formation of the ring-shaped element.

To test the physiological relevance of the dimer of N-domains that is observed in the crystal structure, we determined whether mutation of the critical residue Trp³⁷ to Ala³⁷ (W37A) at the interface would disrupt or reduce oligomerization *in vitro* and transcriptional activation *in vivo*. These experiments were done with STAT-1 (22). Because of the close similarity between the N-domains of STAT-1 and STAT-4 (51% amino acid identity) we expect structural information derived from the STAT-4 crystal structure to represent the STAT-1 architecture as well.

We used an oligonucleotide bearing tandem binding sites that binds two STAT-1 dimers. This site contains two weak binding sites, spaced 10 base pairs apart (23). Competition experiments show that the off time is long for wild-type STAT-1 (greater than 15 to 30 min), indicating the formation of a stable tetrameric complex. In contrast, if an oligonucleotide containing only a single weak site is used instead, the off-time is very short (<30 s) (9). The stabilization of STAT-1 on oligonucleotides containing tandem binding sites is not observed if the N-domain is deleted (9). The W37A mutant protein bound to the DNA probe with tandem sites as a dimer, but the tetrameric interaction was completely displaced by the addition of unlabeled oligonucleotides (Fig. 4A). In contrast, the wild-type protein was resistant to displacement for more than 15 min. We used the same two tandem weak binding sites to drive transcription from a reporter gene in an interferon-dependent transcriptional assay (24) using U3A cells, which lack endogenous STAT-1 (25). In U3A cells transfected with the reporter gene and with either wild-type or W37A mutant STAT-1, the rather weak tran-

scriptional induction of about twofold by interferon γ was abolished by the mutation (Fig. 4B).

Activated and dimeric STAT proteins

do not form detectable tetramers in solution in the absence of DNA (18). It is not known whether this is a consequence of limited binding affinity between N-do-

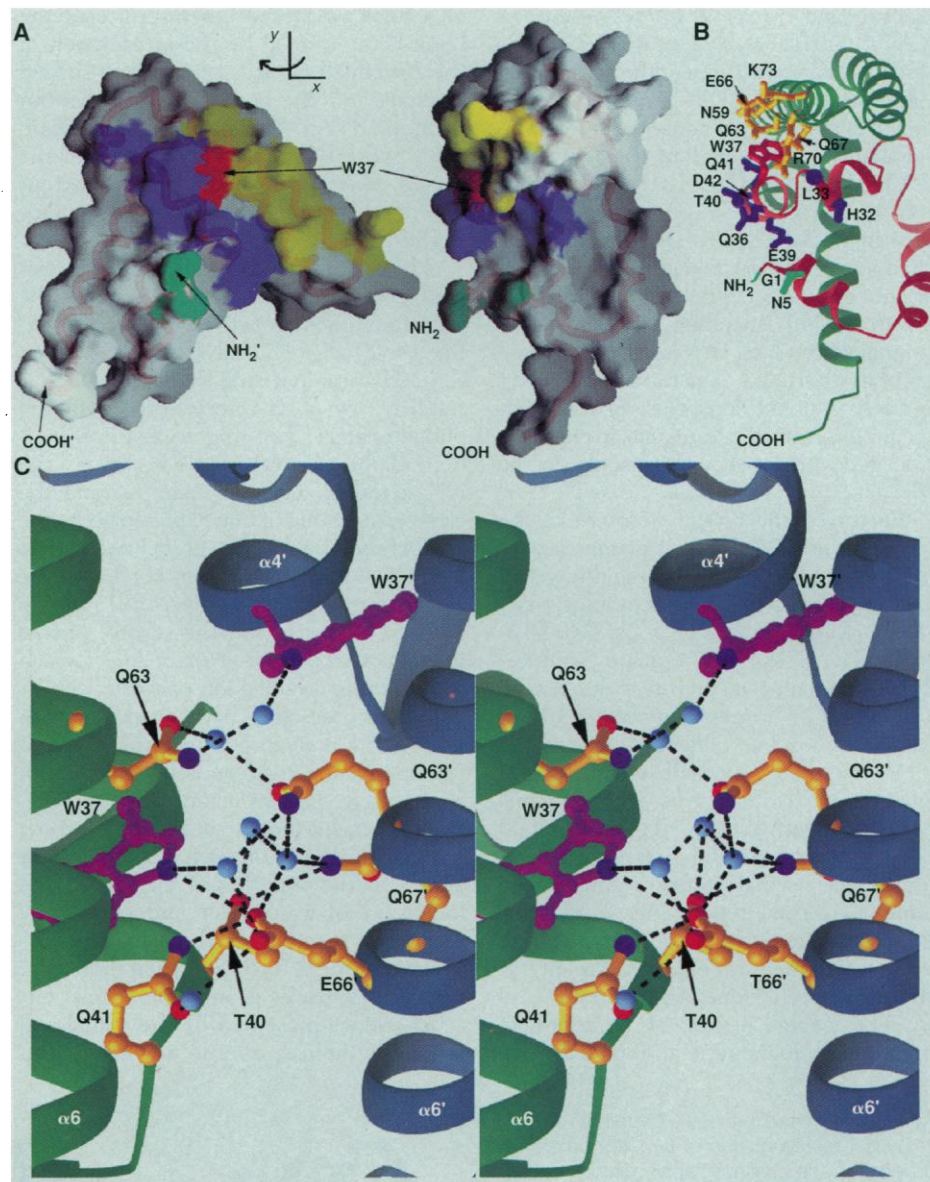


Fig. 3. Structure of the dimer of N-domains. **(A)** Surface representation of the N-domain dimer indicating the wedge-shaped groove and the dimerization interface. Shown are two monomers of a dimer with the left one rotated 90° around the vertical axis away from the original position in the dimer. Note the hook-like appearance of the monomer with the coiled-coil of helices $\alpha 6$ and $\alpha 7$ pointing out of the planar surface formed by the ring-shaped element comprising the NH₂-terminal 40 residues. Residues from three separate regions of the N-domain make direct or water-mediated contacts in the dimer and are color-coded according to their position. Interface residues at the NH₂-terminus are in green, those in helices $\alpha 3$ and $\alpha 4$ are in blue, and amino acids located in helix $\alpha 6$ are yellow. The position of the critical W37 is highlighted in red. The figure was created using GRASP (29). **(B)** A view at the dimerization interface with amino acids represented as ball-and-stick models and the α backbone as a ribbon. The monomer is in the same orientation as the one on the right side of (A). Side chains are colored as in (A); the backbone ribbon is colored as in Fig. 2B, with the first 40 residues highlighted in red. L33 makes a backbone carbonyl group contact, and its position is represented by the filled circle. In the STAT-4 recombinant N-domain used for crystallization, M1 was replaced with G plus four additional small amino acids, one of which (G1) is visible in the electron density map. In the crystals, the NH₂-terminus of G1 is part of the dimer interface, possibly substituting for the native M1. **(C)** Close-up stereoview of the intermolecular hydrogen-bonding network in the dimer. Selected side chains surrounding the conserved W37 (magenta) in helices $\alpha 4$ and $\alpha 6$ of two monomers (green and gray) are shown. W37 makes direct (E66') and water-mediated contacts (Q63'). Water molecules are depicted as blue spheres.

mains or whether the conformation of the STAT molecule in the absence of DNA impedes further oligomerization. In any

case, the presentation of highly polar and unique interaction surfaces by the N-domains of the STATs provides a ready

means for generating very specific interactions between adjacent STAT dimers on DNA, because the hydrogen bonding constraints of the interacting groups place stereochemical constraints on potential partners. Whereas each N-domain dimer is closed, the fact that each STAT dimer presents two N-domains for interaction makes possible the generation of open-ended STAT-STAT interactions that are limited only by the nature and number of the adjacent DNA binding sites.

Fig. 4. Importance of the invariant residue W37 for STAT-1 oligomerization (tetramerization) and mediation of gene activation. **(A)** A gel mobility shift. Comparison of tetramer stability between wild-type (WT) STAT-1 (lanes 3 and 4) and the W37A mutant (lanes 1 and 2). Radiolabeled DNA containing a tandem binding site was incubated with equal amounts of active protein of either Tyr-phosphorylated WT-STAT or the mutant protein and then with excess (30-fold) unlabeled oligonucleotide for the indicated amount of time. Positions of tetrameric [2x(dimer)] and dimeric (Dimer) complexes are indicated. Samples loaded at the later time point (15 min) were subjected to electrophoresis for a shorter time and therefore ran higher on the gel. The position of unbound oligonucleotide (Free) is marked. **(B)** Effect of STAT-1 W37A mutation on interferon- γ (IFN- γ)-stimulated gene activation in vivo. U3A cells were transfected with expression clones containing either wild-type or mutant STAT-1 along with a luciferase reporter containing a tandem STAT-binding site as an enhancer. After stimulation with IFN- γ for 10 hours, luciferase expression was determined spectroscopically. Each bar represents average and standard deviation of 10 individual parallel experiments.

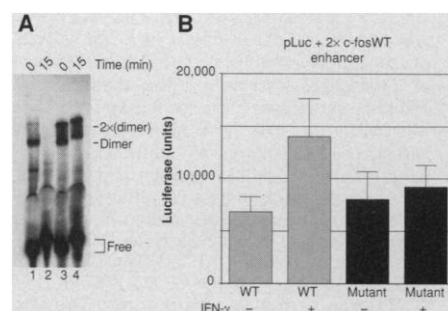


Table 1. Crystallographic analysis. The STAT-1 N-domain formed only small, needle-like crystals. However, hanging drops of STAT-4 N-domain were mixed with equal volumes of reservoir buffer containing 0.2 M Na⁺CH₃COO⁻, 0.1 M tris HCl (pH 8.0), 17% PEG4000, and hexagonal crystals (0.2 mm by 0.2 mm by 0.2 mm) were routinely grown overnight at 20°C. The crystals contain one molecule of the STAT-4 NH₂-terminal domain in the asymmetric unit and are in space group P6₃22 (a = 79.51 Å, b = 79.51 Å, c = 84.68 Å). Crystals were cryoprotected in reservoir solution enriched in PEG to 20% and glycerol to 22.5% before flash-freezing. Heavy-atom derivatives were prepared by soaking crystals for 30 min in a 1:20 diluted (with cryoprotective solution) saturated solution of *p*-hydroxy-mercuribenzoic acid (PHMB). Data for the native crystal were collected at Brookhaven National Laboratory (BNL) at beam-line X25, using a Mar imaging-plate detector system (Mar, Norderstadt, Germany). A multiwavelength anomalous diffraction (MAD) experiment on a PHMB-derivatized crystal was performed at BNL on beam-line X4A, using Fuji imaging plates. Data processing and reduction were done with HKL, DENZO, and SCALEPACK (Z. Otwinowski and W. Minor). Model building was performed with O (30). Bulk solvent correction and anisotropic B-factor scaling was applied during refinement, using X-PLOR (37). Of the five heterologous residues at the NH₂-terminus, the first three residues (GSG), as well as the COOH-terminal residue Q124, are not visible in the electron density map. No amino acids occupy disallowed regions of the ramachandran plot, and 95% fall into the most favored region.

	Resolution (Å)	Reflections (total/unique)	Completeness (%)	R _{sym} * (%)	$\langle I \rangle / \sigma I$
	1.45	237,647/27,594	96.4 (91.7)	7.2 (19.2)	19.6 (4.2)
	Native data				
	MAD analysis‡§				
$\lambda 1 = 1.00842 \text{ \AA}$	2.15	112,445/8854	98.6 (95.7)	7.7 (21.2)	24.7 (6.1)
$\lambda 2 = 1.01337 \text{ \AA}$	2.15	131,403/8992	100.0 (100.0)	7.3 (21.1)	27.2 (8.1)
$\lambda 3 = 1.00932 \text{ \AA}$	2.00	126,292/10,731	96.6 (95.7)	8.4 (33.4)	22.1 (4.5)
Resolution (Å)	Cut-off	Reflections	Completeness (%)	R factor (%)	R free¶ (%)
	Refinement				
10 to 1.45	$ F \sigma(F) > 2$	25,285	88.8	18.8	21.6
10 to 1.45	All data	26,560	93.3	19.4	22.3
rms deviation from ideal stereochemistry					
Bond lengths (Å)		0.015	Water molecules		165
Bond angles (degrees)		1.4	Average B factor (protein) (Å ²)		9.6
			Average B factor (water) (Å ²)		25

*R_{sym} = 100 × $\sum_h \sum_i |I_{hi} - \bar{I}_h| / \sum_h \sum_i I_{hi}$ for the intensity I of i observations of reflection h. For R_{sym} and completeness, the numbers in parentheses refer to data in the shell of highest resolution. I_h is the mean intensity of the reflection. † $\langle I \rangle / \sigma$ = mean intensity/mean SD. ‡Overall mean figure of merit is 0.542 and was calculated from $[\sum P(\alpha)e^{i\alpha} / \sum P(\alpha)]$, where α is the phase and P(α) is the phase distribution probability. §The crystal was derivatized on two sites. ||R factor = 100 × $\sum |F_{obs} - F_{calc}| / \sum |F_{obs}|$, where F_{obs} and F_{calc} are the observed and calculated structure factors, respectively. ¶R free is the same as R factor, but is calculated from the 5% of the reflection data excluded from refinement.

REFERENCES AND NOTES

- D. W. Lbaman, S. Leung, X. Li, G. R. Stark, *FASEB J.* **10**, 1578 (1996); J. E. Darnell Jr., *Science* **277**, 1630 (1997).
- J. E. Darnell Jr., I. M. Kerr, G. R. Stark, *Science* **264**, 1415 (1994).
- C. M. Horvath, Z. Wen, J. E. Darnell Jr., *Genes Dev.* **9**, 984 (1995); H. M. Seidel et al., *Proc. Natl. Acad. Sci. U.S.A.* **92**, 3041 (1995); J. N. Ihle, *Cell* **84**, 331 (1996); T. Mikita, D. Campbell, P. Wu, K. Williamson, U. Schindler, *Mol. Cell. Biol.* **16**, 5811 (1996).
- X. Xu, Y. -L. Sun, T. Hoey, *Science* **273**, 794 (1996).
- V. S. Meier and B. Groner, *Mol. Cell. Biol.* **14**, 128 (1994); A. Symes et al., *Mol. Endocrinol.* **8**, 1750 (1994); M. Dajee et al., *ibid.* **10**, 171 (1996); S. John, C. M. Robbins, W. J. Leonard, *EMBO J.* **15**, 5627 (1996).
- S. L. McKnight, *Genes Dev.* **10**, 367 (1996); R. G. Roeder, *Trends Biochem. Sci.* **21**, 327 (1996).
- R. Tijan and T. Maniatis, *Cell* **77**, 5 (1994).
- S. Leung, X. Li, G. R. Stark, *Science* **273**, 750 (1996).
- U. Vinkemeier et al., *EMBO J.* **15**, 5616 (1996).
- P. L. Bergad, H.-M. Shih, H. C. Towle, S. J. Schwarzenberg, S. A. Berry, *J. Biol. Chem.* **270**, 24903 (1995).
- J. J. Zhang et al., *Proc. Natl. Acad. Sci. U.S.A.* **93**, 15092 (1996).
- S. Leung, S. A. Qureshi, I. M. Kerr, J. E. Darnell Jr., G. R. Stark, *Mol. Cell. Biol.* **15**, 1312 (1995).
- C. Schindler and J. E. Darnell Jr., *Annu. Rev. Biochem.* **64**, 621 (1995).
- X. S. Hou, M. B. Melnick, N. Perrimon, *Cell* **84**, 411 (1996); R. Yan, S. Small, C. Desplan, C. R. Dearolf, J. E. Darnell Jr., *ibid.*, p. 421.
- T. Kawata et al., *ibid.* **89**, 909 (1997).
- R. Yan, H. Luo, J. E. Darnell Jr., C. R. Dearolf, *Proc. Natl. Acad. Sci. U.S.A.* **93**, 5842 (1996).
- The STAT-4 N-domain was expressed as a COOH-terminal fusion with glutathione S-transferase (GST). The expression vector was constructed by amplification in the polymerase chain reaction (PCR; Vent DNA-polymerase, New England Biolabs) of the appropriate region of mouse STAT-4 cDNA and cloning of the fragment into the Bam HI and Eco RI sites of pGEX2T (Pharmacia). Sequence comparison with the STAT-1 N-domain led us to terminate the similar domain in STAT-4 after residue 124. Three glycine residues were included after the thrombin cleavage site [K.-L. Guan and J. E. Dixon, *Anal. Biochem.* **192**, 262 (1991)]. The resulting protein has four additional NH₂-terminal amino acids and Met¹ of STAT-4 is replaced with Gly. The construct was verified by dideoxy sequencing. BL21p(lysS) cells were grown and lysed as described (9). Soluble protein was combined with 0.2 volumes of a 50% (v/v) slurry of glutathione-agarose beads (Pharmacia) and mixed for 5 min. The bound protein was washed with cleavage buffer [50 mM Hepes HCl (pH 8.0), 150 mM KCl, 2.5 mM CaCl₂, and 5 mM dithiothreitol (DTT)]. Cleavage of the GST fusion protein with thrombin (~1 U per milligram of substrate; Novagen) was done overnight at room temperature. Eluted STAT-4 N-domain (in cleavage buffer) was concentrated to 20 mg/ml with centricon (Amicon) and used for crystallization.
- The polymerization status was determined by dynamic light scattering at a protein concentration of

- 1 mg/ml using a Protein Solutions dp801 instrument. [U. Vinkemeier and I. Moarefi, unpublished observations].
19. K. Shuai, J. Y. Liao, M. M. Song, *Mol. Cell. Biol.* **16**, 4932 (1996).
 20. A. Lupas, *Trends Biochem. Sci.* **21**, 375 (1996).
 21. A. R. Fersht *et al.*, *Nature* **314**, 235 (1985); D. Xu, S. L. Lin, R. Nussinov, *J. Mol. Biol.* **265**, 68 (1997).
 22. Tyrosine phosphorylated human wild-type STAT-1 α was produced as described (9). Mutated STAT-1 α (W37A) was expressed from pAcSG2 in baculovirus-infected insect cells. PCR was used to exchange codon 37 [TGG] with [GCA] in the Nco I/Spe I fragment of human STAT-1 cDNA. Additionally, a 6-His tag was added to the COOH-terminus. Modifications were confirmed by sequencing. Insect cells were lysed (dounce homogenizer), and mutated STAT-1 α was purified under native conditions on Ni²⁺ nitrilotriacetic acid (Qiagen) and eluted with 200 mM imidazole in 20 mM Tris HCl (pH 8.0), 10 mM MgCl₂, 50 mM KCl, and 5 mM DTT. In vitro phosphorylation was done as described (9).
 23. Gel-shift experiments and determination of tetramer stability were done as described (9) with an oligonucleotide containing two copies of the STAT recognition element from the c-fos gene (26) spaced by 10 base pairs (5'-GCCAGTCAAGTTCCCGTCAATG-CATCAGGTTCCCGTCAATGCAT-3', binding sites underlined). Both protein preparations (Tyr-phosphorylated wild-type STAT-1 α and W37A mutant) were titrated in gel-shift experiments with an oligonucleotide containing a single M67 (26) site (5'-GCCGATTCCCGTAAATCAT-3') to assure similar loading of active protein.
 24. Transient transfections were done on six-well plates with 50% confluent U3A cells using the calcium phosphate method as instructed by the manufacturer (Stratagene) with the following modifications. Transfection reactions contained 4.5 μ g per well of either wild-type STAT-1 α or the W37A mutant in plasmid pcDNA3 (Invitrogen), 4 μ g of luciferase reporter plasmid pLuc (C. M. Horvath), and 0.4 μ g of β -galactosidase reporter plasmid (Stratagene). The luciferase reporter contained in its Bam HI site as an enhancer element two tandemly arranged weak STAT-1 binding sites (5'-GATCAGTTCCCGTCAATCATGATCCAGTTCCCCGTCAATGATCCCGGATC-3') from the human c-fos promoter. Thirty-six hours after transfection, cells were treated with interferon- γ (5 ng/ml, Amgen) for 10 hours or left untreated. Luciferase assays (Promega) and β -galactosidase assays (Stratagene) were done according to the manufacturer's protocol. Protein expression and Tyr-phosphorylation were checked in gel-shift experiments with whole-cell extracts for both wild-type and mutant protein and were comparable. All results shown are luciferase activities normalized to β -galactosidase activity.
 25. M. Müller *et al.*, *EMBO J.* **12**, 4221 (1993).
 26. B. J. Wagner, T. E. Hayes, C. J. Hoban, B. H. Cochran, *ibid.* **9**, 4477 (1990).
 27. Single-letter abbreviations for the amino acid residues are as follows: A, Ala; C, Cys; D, Asp; E, Glu; F, Phe; G, Gly; H, His; I, Ile; K, Lys; L, Leu; M, Met; N, Asn; P, Pro; Q, Gln; R, Arg; S, Ser; T, Thr; V, Val; W, Trp; and Y, Tyr.
 28. M. Carson, *J. Appl. Crystallogr.* **24**, 958 (1991).
 29. A. Nicholls, K. A. Sharp, B. Honig, *Proteins Struct. Funct. Genet.* **11**, 281 (1991).
 30. T. A. Jones, J. Y. Zou, S. W. Cowan, M. Kjeldgaard, *Acta Crystallogr. A* **47**, 110 (1991).
 31. A. T. Brünger, *X-PLOR (Version 3.1) Manual*, The Howard Hughes Medical Institute and Department of Molecular Biophysics and Biochemistry, Yale University (Yale Univ. Press, New Haven, CT 1992).
 32. We thank H. Viguet and M. M. Allen for expert technical support, X. Zhu and C. M. Horvath for reagents, and the staff at BNL, especially C. Ogata, for advice in collecting MAD data. U.V. expresses special thanks to C. Harrison and F. Sicheri for valuable and generous help with DENZO and X-PLOR, and to D. E. Drake for assistance with figures. Supported by NIH grants AI34420 and AI32489 to J.E.D.

3 September 1997; accepted 10 December 1997

Uncoupling of Immune Complex Formation and Kidney Damage in Autoimmune Glomerulonephritis

Raphael Clynes, Calin Dumitru, Jeffrey V. Ravetch*

The generation of autoantibody and subsequent tissue deposition of immune complexes (IC) is thought to trigger the pathogenic consequences of systemic autoimmune disease. Modulation of the autoantibody response disrupts pathogenesis by preventing the formation of ICs; however, uncoupling IC formation from subsequent inflammatory responses seems unlikely because of the apparent complexity of the IC-triggered inflammatory cascade. However, the disruption of a single gene, which encodes the γ chain of the Fc receptor, was found to achieve this uncoupling in a spontaneous model of lupus nephritis, the New Zealand Black/New Zealand White (NZB/NZW) mouse. Gamma chain-deficient NZB/NZW mice generated and deposited IC and activated complement, but were protected from severe nephritis, thus defining another potential pathway for therapeutic intervention in autoimmune disease.

NZB mice develop autoantibodies and autoimmune hemolytic anemia, but show no signs of glomerular disease until crossed to the NZW background to generate NZB/NZW (B/W F₁) mice (1). A minimum of three distinct genetic loci are required for the manifestation of autoimmune glomerulonephritis in the B/W F₁, two derived from NZB and one from NZW mice (2, 3). Several features of this model are consistent with lupus in humans. Females develop disease at a frequency 10 times that of males, and IC and complement deposition in glomeruli are observed. Significant proteinuria

is seen concomitant with the serological appearance of antibodies to DNA as well as ICs of the immunoglobulin G1 (IgG1), IgG2a, and IgG2b subclasses beginning at 4 months (1). Median survival is 6 months, with mortality resulting from renal failure. Several studies have demonstrated the essential role of B cells (4) and autoantibodies (5, 6) in disease development. Agents that interfere with autoantibody production have been shown to attenuate disease (7–12). Disruption of the subsequent inflammatory response triggered by glomerular IC deposition represents an alternative therapeutic approach, but success may be complicated by the large number of possible proinflammatory molecules presumed to be activated by ICs, including complement components and the cellular receptors for

IgG. Complement depletion attenuates disease in several induced models of glomerulonephritis (13, 14), and anti-C5a treatment modulates glomerular injury in a spontaneous murine model (15). However, the primacy of complement activation in IC-triggered inflammation has been questioned by several recent genetic studies (16–20).

In the classical model of IC-triggered inflammation, the Arthus reaction, the demonstration that Fc γ Rs are essential whereas complement is not (16–20) suggests that the fundamental assumption of the pathogenesis of autoimmune glomerulonephritis as being mediated by complement activation (13, 21–27) requires re-evaluation. Such studies have been facilitated by the availability of defined murine strains deficient in components of this pathway. Mouse strain $\gamma^{-/-}$, which is deficient in the Fc receptor (FcR) γ chain, does not express the activation receptors Fc γ RI and Fc γ RIII, but still bears the inhibitory receptor Fc γ RIIB. To determine if the spontaneous autoimmune glomerulonephritis in the B/W F₁ required Fc γ Rs for disease development, NZB and NZW mice were backcrossed for eight generations to the $\gamma^{-/-}$ mouse strain, and animals homozygous or heterozygous for the disruption in the γ chain were identified. We obtained $\gamma^{+/-}$ and $\gamma^{-/-}$ B/W F₁ animals and observed them for evidence of autoimmune glomerulonephritis. As reported (1), B/W F₁ animals have a median survival of 200 days, succumbing to the sequelae of renal failure (Fig. 1A). In contrast, $\gamma^{-/-}$ B/W mice had a prolonged survival, with 82% (20 of 22) alive at 9 months. In B/W mice, the appearance of proteinuria presages the onset of

Laboratory of Molecular Genetics and Immunology, The Rockefeller University, New York, NY 10021, USA.

*To whom correspondence should be addressed. E-mail: ravetch@rockefeller.edu